Measurements of the Top-quark Mass and the $t\bar{t}$ Cross Section in the Hadronic τ + Jets Decay Channel at $\sqrt{s} = 1.96$ TeV

T. Aaltonen,[21] B. Álvarez González[z],[9] S. Amerio,[40] D. Amidei,[32] A. Anastassov[x],[15] A. Annovi,[17] J. Antos,[12] G. Apollinari,[15] J.A. Appel,[15] T. Arisawa,[54] A. Artikov,[13] J. Asaadi,[49] W. Ashmanskas,[15] B. Auerbach,[57] A. Aurisano,[49] F. Azfar,[39] W. Badgett,[15] T. Bae,[25] A. Barbaro-Galtieri,[26] V.E. Barnes,[44] B.A. Barnett,[23] P. Barria[hh],[42] P. Bartos,[12] M. Bauce[ff],[40] F. Bedeschi,[42] S. Behari,[23] G. Bellettini[gg],[42] J. Bellinger,[56] D. Benjamin,[14] A. Beretvas,[15] A. Bhatti,[46] D. Bisello[ff],[40] I. Bizjak,[28] K.R. Bland,[5] B. Blumenfeld,[23] A. Bocci,[14] A. Bodek,[45] D. Bortoletto,[44] J. Boudreau,[43] A. Boveia,[11] L. Brigliadori[ee],[6] C. Bromberg,[33] E. Brucken,[21] J. Budagov,[13] H.S. Budd,[45] K. Burkett,[15] G. Busetto[ff],[40] P. Bussey,[19] A. Buzatu,[31] A. Calamba,[10] C. Calancha,[29] S. Camarda,[4] M. Campanelli,[28] M. Campbell,[32] F. Canelli[11],[15] B. Carls,[22] D. Carlsmith,[56] R. Carosi,[42] S. Carrillo[m],[16] S. Carron,[15] B. Casal[k],[9] M. Casarsa,[50] A. Castro[ee],[6] P. Catastini,[20] D. Cauz,[50] V. Cavaliere,[22] M. Cavalli-Sforza,[4] A. Cerri[f],[26] L. Cerrito[s],[28] Y.C. Chen,[1] M. Chertok,[7] G. Chiarelli,[42] G. Chlachidze,[15] F. Chlebana,[15] K. Cho,[25] D. Chokheli,[13] W.H. Chung,[56] Y.S. Chung,[45] M.A. Ciocci[hh],[42] A. Clark,[18] C. Clarke,[55] G. Compostella[ff],[40] M.E. Convery,[15] J. Conway,[7] M.Corbo,[15] M. Cordelli,[17] C.A. Cox,[7] D.J. Cox,[7] F. Crescioli[gg],[42] J. Cuevas[z],[9] R. Culbertson,[15] D. Dagenhart,[15] N. d'Ascenzo[w],[15] M. Datta,[15] P. de Barbaro,[45] M. Dell'Orso[gg],[42] L. Demortier,[46] M. Deninno,[6] F. Devoto,[21] M. d'Errico[ff],[40] A. Di Canto[gg],[42] B. Di Ruzza,[15] J.R. Dittmann,[5] M. D'Onofrio,[27] S. Donati[gg],[42] P. Dong,[15] M. Dorigo,[50] T. Dorigo,[40] K. Ebina,[54] A. Elagin,[49] A. Eppig,[32] R. Erbacher,[7] S. Errede,[22] N. Ershaidat[dd],[15] R. Eusebi,[49] S. Farrington,[39] M. Feindt,[24] J.P. Fernandez,[29] R. Field,[16] G. Flanagan[u],[15] R. Forrest,[7] M.J. Frank,[5] M. Franklin,[20] J.C. Freeman,[15] Y. Funakoshi,[54] I. Furic,[16] M. Gallinaro,[46] J.E. Garcia,[18] A.F. Garfinkel,[44] P. Garosi[hh],[42] H. Gerberich,[22] E. Gerchtein,[15] S. Giagu,[47] V. Giakoumopoulou,[3] P. Giannetti,[42] K. Gibson,[43] C.M. Ginsburg,[15] N. Giokaris,[3] P. Giromini,[17] G. Giurgiu,[23] V. Glagolev,[13] D. Glenzinski,[15] M. Gold,[35] D. Goldin,[49] N. Goldschmidt,[16] A. Golossanov,[15] G. Gomez,[9] G. Gomez-Ceballos,[30] M. Goncharov,[30] O. González,[29] I. Gorelov,[35] A.T. Goshaw,[14] K. Goulianos,[46] S. Grinstein,[4] C. Grosso-Pilcher,[11] R.C. Group[53],[15] J. Guimaraes da Costa,[20] S.R. Hahn,[15] E. Halkiadakis,[48] A. Hamaguchi,[38] J.Y. Han,[45] F. Happacher,[17] K. Hara,[51] D. Hare,[48] M. Hare,[52] R.F. Harr,[55] K. Hatakeyama,[5] C. Hays,[39] M. Heck,[24] J. Heinrich,[41] M. Herndon,[56] S. Hewamanage,[5] A. Hocker,[15] W. Hopkins[g],[15] D. Horn,[24] S. Hou,[1] R.E. Hughes,[36] M. Hurwitz,[11] U. Husemann,[57] N. Hussain,[31] M. Hussein,[33] J. Huston,[33] G. Introzzi,[42] M. Iori[jj],[47] A. Ivanov[p],[7] E. James,[15] D. Jang,[10] B. Jayatilaka,[14] E.J. Jeon,[25] S. Jindariani,[15] M. Jones,[44] K.K. Joo,[25] S.Y. Jun,[10] T.R. Junk,[15] T. Kamon[25],[49] P.E. Karchin,[55] A. Kasmi,[5] Y. Kato[o],[38] W. Ketchum,[11] J. Keung,[41] V. Khotilovich,[49] B. Kilminster,[15] D.H. Kim,[25] H.S. Kim,[25] J.E. Kim,[25] M.J. Kim,[17] S.B. Kim,[25] S.H. Kim,[51] Y.K. Kim,[11] Y.J. Kim,[25] N. Kimura,[54] M. Kirby,[15] S. Klimenko,[16] K. Knoepfel,[15] K. Kondo,[54] D.J. Kong,[25] J. Konigsberg,[16] A.V. Kotwal,[14] M. Kreps,[24] J. Kroll,[41] D. Krop,[11] M. Kruse,[14] V. Krutelyov[c],[49] T. Kuhr,[24] M. Kurata,[51] S. Kwang,[11] A.T. Laasanen,[44] S. Lami,[42] S. Lammel,[15] M. Lancaster,[28] R.L. Lander,[7] K. Lannon[y],[36] A. Lath,[48] G. Latino[hh],[42] T. LeCompte,[2] E. Lee,[49] H.S. Lee[q],[11] J.S. Lee,[25] S.W. Lee[bb],[49] S. Leo[gg],[42] S. Leone,[42] J.D. Lewis,[15] A. Limosani[t],[14] C.-J. Lin,[26] M. Lindgren,[15] E. Lipeles,[41] A. Lister,[18] D.O. Litvintsev,[15] C. Liu,[43] H. Liu,[53] Q. Liu,[44] T. Liu,[15] S. Lockwitz,[57] A. Loginov,[57] D. Lucchesi[ff],[40] J. Lueck,[24] P. Lujan,[26] P. Lukens,[15] G. Lungu,[46] J. Lys,[26] R. Lysak[e],[12] R. Madrak,[15] K. Maeshima,[15] P. Maestro[hh],[42] S. Malik,[46] G. Manca[a],[27] A. Manousakis-Katsikakis,[3] F. Margaroli,[47] C. Marino,[24] M. Martínez,[4] P. Mastrandrea,[47] K. Matera,[22] M.E. Mattson,[55] A. Mazzacane,[15] P. Mazzanti,[6] K.S. McFarland,[45] P. McIntyre,[49] R. McNulty[j],[27] A. Mehta,[27] P. Mehtala,[21] C. Mesropian,[46] T. Miao,[15] D. Mietlicki,[32] A. Mitra,[1] H. Miyake,[51] S. Moed,[15] N. Moggi,[6] M.N. Mondragon[m],[15] C.S. Moon,[25] R. Moore,[15] M.J. Morello[ii],[42] J. Morlock,[24] P. Movilla Fernandez,[15] A. Mukherjee,[15] Th. Muller,[24] P. Murat,[15] M. Mussini[ee],[6] J. Nachtman[n],[15] Y. Nagai,[51] J. Naganoma,[54] I. Nakano,[37] A. Napier,[52] J. Nett,[49] C. Neu,[53] M.S. Neubauer,[22] J. Nielsen[d],[26] L. Nodulman,[2] S.Y. Noh,[25] O. Norniella,[22] L. Oakes,[39] S.H. Oh,[14] Y.D. Oh,[25] I. Oksuzian,[53] T. Okusawa,[38] R. Orava,[21] L. Ortolan,[4] S. Pagan Griso[ff],[40] C. Pagliarone,[50] E. Palencia[f],[9] V. Papadimitriou,[15] A.A. Paramonov,[2] J. Patrick,[15] G. Pauletta[kk],[50] M. Paulini,[10] C. Paus,[30] D.E. Pellett,[7] A. Penzo,[50] T.J. Phillips,[14] G. Piacentino,[42] E. Pianori,[41] J. Pilot,[36] K. Pitts,[22] C. Plager,[8] L. Pondrom,[56] S. Poprocki[g],[15] K. Potamianos,[44] F. Prokoshin[cc],[13] F. Ptohos[h],[17] G. Punzi[gg],[42] A. Rahaman,[43] V. Ramakrishnan,[56] N. Ranjan,[44] I. Redondo,[29] P. Renton,[39] M. Rescigno,[47] T. Riddick,[28] F. Rimondi[ee],[6] L. Ristori[42],[15] A. Robson,[19] T. Rodrigo,[9] T. Rodriguez,[41] E. Rogers,[22] S. Rolli[i],[52] R. Roser,[15] F. Ruffini[hh],[42] A. Ruiz,[9] J. Russ,[10] V. Rusu,[15] A. Safonov,[49] W.K. Sakumoto,[45] Y. Sakurai,[54] L. Santi[kk],[50] K. Sato,[51]

V. Saveliev[w],[15] A. Savoy-Navarro[aa],[15] P. Schlabach,[15] A. Schmidt,[24] E.E. Schmidt,[15] T. Schwarz,[15] L. Scodellaro,[9] A. Scribano[hh],[42] F. Scuri,[42] S. Seidel,[35] Y. Seiya,[38] A. Semenov,[13] F. Sforza[hh],[42] S.Z. Shalhout,[7] T. Shears,[27] P.F. Shepard,[43] M. Shimojima[v],[51] M. Shochet,[11] I. Shreyber-Tecker,[34] A. Simonenko,[13] P. Sinervo,[31] K. Sliwa,[52] J.R. Smith,[7] F.D. Snider,[15] A. Soha,[15] V. Sorin,[4] H. Song,[43] P. Squillacioti[hh],[42] M. Stancari,[15] R. St. Denis,[19] B. Stelzer,[31] O. Stelzer-Chilton,[31] D. Stentz[x],[15] J. Strologas,[35] G.L. Strycker,[32] Y. Sudo,[51] A. Sukhanov,[15] I. Suslov,[13] K. Takemasa,[51] Y. Takeuchi,[51] J. Tang,[11] M. Tecchio,[32] P.K. Teng,[1] J. Thom[g],[15] J. Thome,[10] G.A. Thompson,[22] E. Thomson,[41] D. Toback,[49] S. Tokar,[12] K. Tollefson,[33] T. Tomura,[51] D. Tonelli,[15] S. Torre,[17] D. Torretta,[15] P. Totaro,[40] M. Trovato[ii],[42] F. Ukegawa,[51] S. Uozumi,[25] A. Varganov,[32] F. Vázquez[m],[16] G. Velev,[15] C. Vellidis,[15] M. Vidal,[44] I. Vila,[9] R. Vilar,[9] J. Vizán,[9] M. Vogel,[35] G. Volpi,[17] P. Wagner,[41] R.L. Wagner,[15] T. Wakisaka,[38] R. Wallny,[8] S.M. Wang,[1] A. Warburton,[31] D. Waters,[28] W.C. Wester III,[15] D. Whiteson[b],[41] A.B. Wicklund,[2] E. Wicklund,[15] S. Wilbur,[11] F. Wick,[24] H.H. Williams,[41] J.S. Wilson,[36] P. Wilson,[15] B.L. Winer,[36] P. Wittich[g],[15] S. Wolbers,[15] H. Wolfe,[36] T. Wright,[32] X. Wu,[18] Z. Wu,[5] K. Yamamoto,[38] D. Yamato,[38] T. Yang,[15] U.K. Yang[r],[11] Y.C. Yang,[25] W.-M. Yao,[26] G.P. Yeh,[15] K. Yi[n],[15] J. Yoh,[15] K. Yorita,[54] T. Yoshida[l],[38] G.B. Yu,[14] I. Yu,[25] S.S. Yu,[15] J.C. Yun,[15] A. Zanetti,[50] Y. Zeng,[14] C. Zhou,[14] and S. Zucchelli[ee][6]

(CDF Collaboration)

[1]Institute of Physics, Academia Sinica, Taipei, Taiwan 11529, Republic of China
[2]Argonne National Laboratory, Argonne, Illinois 60439, USA
[3]University of Athens, 157 71 Athens, Greece
[4]Institut de Fisica d'Altes Energies, ICREA, Universitat Autonoma de Barcelona, E-08193, Bellaterra (Barcelona), Spain
[5]Baylor University, Waco, Texas 76798, USA
[6]Istituto Nazionale di Fisica Nucleare Bologna, [ee]University of Bologna, I-40127 Bologna, Italy
[7]University of California, Davis, Davis, California 95616, USA
[8]University of California, Los Angeles, Los Angeles, California 90024, USA
[9]Instituto de Fisica de Cantabria, CSIC-University of Cantabria, 39005 Santander, Spain
[10]Carnegie Mellon University, Pittsburgh, Pennsylvania 15213, USA
[11]Enrico Fermi Institute, University of Chicago, Chicago, Illinois 60637, USA
[12]Comenius University, 842 48 Bratislava, Slovakia; Institute of Experimental Physics, 040 01 Kosice, Slovakia
[13]Joint Institute for Nuclear Research, RU-141980 Dubna, Russia
[14]Duke University, Durham, North Carolina 27708, USA
[15]Fermi National Accelerator Laboratory, Batavia, Illinois 60510, USA
[16]University of Florida, Gainesville, Florida 32611, USA
[17]Laboratori Nazionali di Frascati, Istituto Nazionale di Fisica Nucleare, I-00044 Frascati, Italy
[18]University of Geneva, CH-1211 Geneva 4, Switzerland
[19]Glasgow University, Glasgow G12 8QQ, United Kingdom
[20]Harvard University, Cambridge, Massachusetts 02138, USA
[21]Division of High Energy Physics, Department of Physics,
University of Helsinki and Helsinki Institute of Physics, FIN-00014, Helsinki, Finland
[22]University of Illinois, Urbana, Illinois 61801, USA
[23]The Johns Hopkins University, Baltimore, Maryland 21218, USA
[24]Institut für Experimentelle Kernphysik, Karlsruhe Institute of Technology, D-76131 Karlsruhe, Germany
[25]Center for High Energy Physics: Kyungpook National University,
Daegu 702-701, Korea; Seoul National University, Seoul 151-742,
Korea; Sungkyunkwan University, Suwon 440-746,
Korea; Korea Institute of Science and Technology Information,
Daejeon 305-806, Korea; Chonnam National University, Gwangju 500-757,
Korea; Chonbuk National University, Jeonju 561-756, Korea
[26]Ernest Orlando Lawrence Berkeley National Laboratory, Berkeley, California 94720, USA
[27]University of Liverpool, Liverpool L69 7ZE, United Kingdom
[28]University College London, London WC1E 6BT, United Kingdom
[29]Centro de Investigaciones Energeticas Medioambientales y Tecnologicas, E-28040 Madrid, Spain
[30]Massachusetts Institute of Technology, Cambridge, Massachusetts 02139, USA
[31]Institute of Particle Physics: McGill University, Montréal, Québec,
Canada H3A 2T8; Simon Fraser University, Burnaby, British Columbia,
Canada V5A 1S6; University of Toronto, Toronto, Ontario,
Canada M5S 1A7; and TRIUMF, Vancouver, British Columbia, Canada V6T 2A3
[32]University of Michigan, Ann Arbor, Michigan 48109, USA
[33]Michigan State University, East Lansing, Michigan 48824, USA
[34]Institution for Theoretical and Experimental Physics, ITEP, Moscow 117259, Russia
[35]University of New Mexico, Albuquerque, New Mexico 87131, USA
[36]The Ohio State University, Columbus, Ohio 43210, USA

[37] Okayama University, Okayama 700-8530, Japan
[38] Osaka City University, Osaka 588, Japan
[39] University of Oxford, Oxford OX1 3RH, United Kingdom
[40] Istituto Nazionale di Fisica Nucleare, Sezione di Padova-Trento, [ff] University of Padova, I-35131 Padova, Italy
[41] University of Pennsylvania, Philadelphia, Pennsylvania 19104, USA
[42] Istituto Nazionale di Fisica Nucleare Pisa, [gg] University of Pisa,
[hh] University of Siena and [ii] Scuola Normale Superiore, I-56127 Pisa, Italy
[43] University of Pittsburgh, Pittsburgh, Pennsylvania 15260, USA
[44] Purdue University, West Lafayette, Indiana 47907, USA
[45] University of Rochester, Rochester, New York 14627, USA
[46] The Rockefeller University, New York, New York 10065, USA
[47] Istituto Nazionale di Fisica Nucleare, Sezione di Roma 1,
[jj] Sapienza Università di Roma, I-00185 Roma, Italy
[48] Rutgers University, Piscataway, New Jersey 08855, USA
[49] Texas A&M University, College Station, Texas 77843, USA
[50] Istituto Nazionale di Fisica Nucleare Trieste/Udine,
I-34100 Trieste, [kk] University of Udine, I-33100 Udine, Italy
[51] University of Tsukuba, Tsukuba, Ibaraki 305, Japan
[52] Tufts University, Medford, Massachusetts 02155, USA
[53] University of Virginia, Charlottesville, Virginia 22906, USA
[54] Waseda University, Tokyo 169, Japan
[55] Wayne State University, Detroit, Michigan 48201, USA
[56] University of Wisconsin, Madison, Wisconsin 53706, USA
[57] Yale University, New Haven, Connecticut 06520, USA
(Dated: August 23, 2012)

We present the first direct measurement of the top-quark mass using $t\bar{t}$ events decaying in the hadronic τ + jets decay channel. Using data corresponding to an integrated luminosity of 2.2 fb^{-1} collected by the CDF II detector in $p\bar{p}$ collisions at $\sqrt{s}$ = 1.96 TeV at the Fermilab Tevatron, we measure the $t\bar{t}$ cross section, $\sigma_{t\bar{t}}$, and the top-quark mass, M_{top}. We extract M_{top} from a likelihood based on per-event probabilities calculated with leading-order signal and background matrix elements. We measure $\sigma_{t\bar{t}} = 8.8 \pm 3.3$ (stat) ± 2.2 (syst) pb and $M_{\text{top}} = 172.7 \pm 9.3$ (stat) $\pm$ 3.7 (syst) GeV/c^2.

The mass of the top quark, M_{top}, and the top-quark pair production cross section, $\sigma_{t\bar{t}}$, have been extensively studied at both the Fermilab Tevatron and the Large Hadron Collider at CERN [1–3]. However, final states of the top-quark decay that include a tau lepton (τ) are relatively unexplored due to the difficulty of identifying the tau and rejecting quantum chromodynamic (QCD) processes that can mimic its hadronic decay mode. The top quark and the tau belong to the heaviest third generation of standard model (SM) fermions and may play a special role in electroweak symmetry breaking. Measurements in these unexplored decay channels serve as important tests of lepton universality, and discrepancies from the SM expectation could point to new top-quark sector physics.

In this Letter, we present the first direct measurement of the top-quark mass in the hadronic τ + jets decay channel (τ + jets) [4]. We measure $\sigma_{t\bar{t}}$ and M_{top} using data corresponding to 2.2 fb^{-1} of integrated luminosity collected by the CDF II detector [5] in $p\bar{p}$ collisions at $\sqrt{s}$ = 1.96 TeV at the Fermilab Tevatron. The D0 Collaboration previously measured $\sigma_{t\bar{t}}$ in the τ + jets decay channel with data corresponding to 1 fb^{-1} of integrated luminosity to be 6.9 ± 1.5 pb [6], assuming $M_{\text{top}} = 170$ GeV/c^2, and reached a signal purity of 52%.

Assuming three generations in the SM and a unitary quark-mixing matrix, the top quark decays almost exclusively to a W boson and b quark. We select pair-produced top-quark events in which one of the W bosons decays into a pair of light quarks and the other decays to a tau and a neutrino. This decay channel represents 15.2% of the $t\bar{t}$ branching ratio and results in a final state with a tau, a neutrino, two b quarks, and two light-flavor quarks (u, d, or s). Although the tau can decay leptonically to an electron (e) or muon (μ) and a pair of neutrinos, these events are difficult to differentiate from electrons or muons from W boson decays. As a result, we select events with the tau decaying to a neutrino and a narrow jet of hadrons, which are usually charged and neutral pions, that correspond to 9.8% of all $t\bar{t}$ decays. We use an artificial neural network (NN) to reduce the QCD multijet background contribution. The additional neutrino produced in the tau decay complicates the tau reconstruction. To solve this, we adapt a missing mass calculator method [7] to the τ + jets topology to infer a unique solution for the neutrino four-momentum with sufficient precision to reasonably reconstruct the tau. We use a binned likelihood fit based on the predicted and ob-

served number of events to measure $\sigma_{t\bar{t}}$. Then, to extract M_{top}, we use a likelihood function built from signal and background probabilities calculated with the predicted differential cross sections for $t\bar{t}$ and W + four-parton production, respectively.

The data used in this measurement are selected using a multijet online selection (trigger) that requires at least four calorimeter energy clusters with transverse energy [8] (E_T) greater than 15 GeV each and a total sum E_T of all clusters greater than 175 GeV [9]. Jets are reconstructed by a cone algorithm that clusters energies in calorimeter towers within a fixed cone size of $\Delta R = 0.4$ [10] where $\Delta R = \sqrt{\Delta \eta^2 + \Delta \phi^2}$ [8]. In the offline analysis, events are required to have exactly four jets with $E_T > 20$ GeV, missing transverse energy ($\not{E}_T$) greater than 20 GeV, and a single hadronically-decaying tau selected as described below. Jet energies are corrected for nonlinearity of the detector response and multiple $p\bar{p}$ interactions within the bunch crossing [11]. One of the four jets must be identified as having originated from a b quark (b-tagged) using a secondary vertex finding algorithm [12]. Hadronically-decaying taus appear as narrow jets with an odd number of tracks and low neutral pion multiplicity. We select taus using a two-cones algorithm [13]. The inner cone defining the signal region has a size set to the lesser of 10° (0.17 rad) and (5 GeV)/E_{cl} rad, where E_{cl} is the energy of the calorimeter energy cluster associated with the tau candidate. The second cone with a size of 30° defines an isolation region outside of the signal cone. A tau must have one or three tracks in the signal region and no tracks in the isolation region. We require the E_T of the tau energy cluster to exceed 20 GeV and the E_T of the visible tau to exceed 25 GeV, where visible refers to the combination of the track and neutral pion information. We require that the calorimeter energy in the isolation region be less than 10% of the visible tau energy. Finally, we veto events with an identified electron or muon.

The dominant background for this analysis is high jet multiplicity QCD events with a jet misidentified as a tau. To reduce this background, we develop a NN to distinguish between $t\bar{t} \rightarrow \tau$ + jets and QCD multijet events. The NN is trained using QCD multijet events, obtained from data by selecting events with a tau candidate with at least one track in the isolation region and passing all other selection requirements, and $t\bar{t}$ events generated using the PYTHIA Monte Carlo generator [14] coupled with a GEANT [15] based CDF II detector simulation [16]. To properly account for tau polarization effects, the tau decays are modeled by the TAUOLA package [17]. The NN uses eight variables that exploit the topological differences between QCD multijet and $t\bar{t}$ events including $\not{E}_T$ and the sum of the E_T of various combinations of the tau and jets [4]. After training the NN, we find good separation between QCD multijet and $t\bar{t}$ events. Optimal signal significance, defined as the number of expected signal events divided by the square root of the total number of observed events, is achieved by removing events associated to a NN value below 0.85. We initially select 162 events of which 41 events survive the 0.85 NN requirement. Due to the difficulty in simulating QCD multijet events, b quark tagging algorithms, and the production of heavy flavor quarks in association with W bosons, we estimate the background contributions with a data-driven approach similar to that described in Ref. [12]. We use the NN output distribution to fit the contributions of the signal and background processes to the data. This is done both before and after applying b-tagging requirements. Since most of the selected data events return a NN value below 0.7, the fit is dominated by events outside of the signal region. We begin by calculating the contributions of the signal and each background process before the b-tagging requirement is applied. The $t\bar{t}$ and electroweak background contributions are determined from simulation.

Diboson, single top-quark, and Z + jets production are modeled using PYTHIA, MADEVENT [18], and ALPGEN [19] respectively, with PYTHIA used for parton showering and underlying event generation. Each of these processes' contributions is set to its expectation based on its respective theoretical cross section [20, 21], the total integrated luminosity of the data, and the acceptance determined from simulation. The $t\bar{t}$ contribution is modeled with PYTHIA and is similarly normalized using the next-to-next-to-leading order SM $t\bar{t}$ cross section prediction [22]. For all simulated events, a GEANT based simulation is used to model the CDF II detector response. With these contributions known, we determine the contributions from QCD multijet and W + jets events by fitting the shape of the NN output distribution for each component (with the previously calculated contributions fixed) to the data before applying the NN selection and b-tagging requirements. The QCD multijet sample is selected from data as previously described while the W + jets events are modeled with ALPGEN similarly to Z + jets events. We fit these distributions with a binned Poisson likelihood as seen in Fig. 1. The contribution of QCD multijet events in the signal region is calculated from this fit. All remaining events are assumed to come from W + jets production.

For each process except QCD multijet events, the contribution after applying the b-tagging requirement is calculated by applying b-tagging efficiencies measured in Ref. [12] to the initially calculated contribution. Incorrect tagging of light quarks and tagging of the b and c quarks have inherently different uncertainties. To properly estimate uncertainties associated with the contribution of W + jets events, this contribution is divided into W + light flavor (W+lf) and W + heavy flavor ($Wb\bar{b}$, $Wc\bar{c}$, and Wc) parts with separately-estimated uncertainties. To calculate the contribution from QCD multijet events, we apply the b-tagging requirement to the

TABLE I. Predicted number of selected τ + jets candidate events from each considered process after all selection requirements are applied assuming $\sigma_{t\bar{t}} = 7.4$ pb and $M_{\text{top}} = 172.5$ GeV/c^2. The uncertainty is a combination of statistical and systematic uncertainty.

Source	Number of events
Diboson	0.19 ± 0.01
Single top quark	0.16 ± 0.01
$Zb\bar{b}$	0.29 ± 0.04
$Wb\bar{b}$	0.6 ± 0.5
$Wc\bar{c}$	0.3 ± 0.3
Wc	0.2 ± 0.1
W+lf	0.5 ± 0.6
QCD multijet	18.2 ± 4.1
Total bkgd	20.4 ± 4.2
$t\bar{t}$	18.2 ± 2.8
Total predicted	38.6 ± 5.0
Observed	41

QCD multijet sample. We then combine $t\bar{t}$ and the other background processes into a single sample with the relative contributions fixed to their calculated values. The NN output distributions of these two samples are then fit to the data selected with the b-tagging requirement, and the contribution of QCD multijet events in the signal region is derived from the result. Each process's contribution, assuming $\sigma_{t\bar{t}} = 7.4$ pb and $M_{\text{top}} = 172.5$ GeV/c^2, is given in Table I. Of the 41 selected events, we expect roughly 18 QCD multijet events and 18 $t\bar{t}$ events. From simulation studies, we estimate that $76.5 \pm 0.5\%$ of the selected $t\bar{t}$ events correspond to a hadronic τ + jets final state. The other major contributions to the $t\bar{t}$ events are all-hadronic $t\bar{t}$ decays ($12.3 \pm 0.4\%$) and $t\bar{t} \to e$ + jets ($5.3 \pm 0.3\%$).
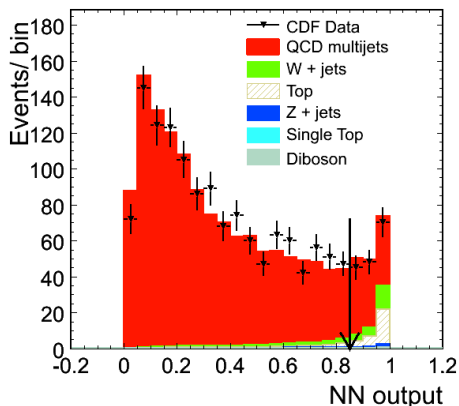

FIG. 1. Fit to the NN output shape before applying the b-tagging requirement. The arrow marks the lower bound on the signal region.

We measure $\sigma_{t\bar{t}}$ using a likelihood function based on a Poisson probability distribution comparing the number of observed (N_o) and predicted (N_p) events for a given $\sigma_{t\bar{t}}$ written as $L = e^{-N_p} N_p^{N_o}/(N_o!)$. We consider the negative logarithm of this function over values of $\sigma_{t\bar{t}}$ from 5 to 15 pb where N_p is recalculated at each point with the fraction of QCD multijet events kept constant to the value calculated for $\sigma_{t\bar{t}} = 7.4$ pb. The result is fit with a 2nd order polynomial which is minimized to extract the central value and statistical uncertainty. The cross section value determined by the fit is $\sigma_{t\bar{t}} = 8.8 \pm 3.3$ (stat) pb.

The dominant sources of systematic uncertainty include the acceptance, selection efficiencies, background estimate, and luminosity. For acceptance effects, we consider uncertainties on the jet energy scale (JES) [11] (0.6 pb), parton showering models (0.5 pb), parton distribution functions (PDF) (0.5 pb), initial and final state radiation (ISR, FSR) (0.5 pb), and color reconnection [23] (0.4 pb). We consider systematic uncertainties on the efficiency measurements from the b-tagging (0.4 pb), tau identification (0.2 pb), and trigger efficiency (0.1 pb) scale factors. The background systematics come from the W + heavy flavor scale factor uncertainty [12] (0.1 pb) and the QCD multijet contribution, which is the dominant systematic uncertainty. We measure this uncertainty (1.8 pb) by comparing the NN output distribution shapes of the QCD multijet events and data dominated by QCD multijet events which are selected by removing the $\not{E}_{\text{T}}$ requirement. Finally, the uncertainty on the integrated luminosity is 6% [24] (0.5 pb). Combining all these sources in quadrature results in the total systematic uncertainty of 2.2 pb, a 25% uncertainty. We measure $\sigma_{t\bar{t}}$ assuming $M_{\text{top}} = 172.5$ GeV/c^2 to be 8.8 ± 3.3 (stat) ± 2.2 (syst) pb, which is consistent with the next-to-next-to-leading order SM prediction of $7.45^{+0.72}_{-0.63}$ pb [22].

We calculate M_{top} from a likelihood function based on probabilities corresponding to the signal and background hypothesis for each event. These probabilities are calculated from the differential cross section for $t\bar{t}$ and W + four-parton production, respectively. The method uses a similar approach to the previous measurement in the e and μ + jets decay channels [25]. The signal probability is based on a $t\bar{t}$ leading-order matrix element which assumes $q\bar{q}$ production [26] and is calculated over 31 input mass values ranging from 145 to 205 GeV/c^2. Since it does not depend on M_{top}, the background probability is calculated once for each event using a W + four-parton matrix element from the vecbos [27] generator.

The tau decay adds an extra complication by introducing a second neutrino in the event. We reconstruct this additional neutrino by adapting a method developed for the reconstruction of a resonance decaying to $\tau\tau$ [7] to the τ + jets topology. We find from simulation studies of $t\bar{t} \to \tau$ + jets events that the neutrino from the tau

decay is nearly collinear with the hadronic components of the tau decay as their θ and ϕ angles tend to agree within 0.1 radians. Additionally, we find that the ϕ angle of the neutrino from the W boson is within 1 radian of the ϕ direction associated with the $\not{E}_T$. Simulation studies show that these statements hold true in greater than 99% of events. We introduce a four-dimensional scan over the angles of both neutrinos restricting them to the above ranges. Assuming the neutrino mass is negligible and that the W boson and tau have masses of 80.4 GeV/c^2 and 1.777 GeV/c^2, respectively, we completely solve for the four-vector of each neutrino for each set of angles in the scan. We then compare the predicted x- and y-components of the $\not{E}_T$ from the neutrino solutions to the measured $\not{E}_T$ components with Gaussian probability functions and choose the set of angles that returns the greatest probability. This method accurately reconstructs the four-momentum of the neutrino from the tau decay, but it does not perform as well with the four-momentum of the neutrino from the W boson decay. Therefore, we use the result of this method only to determine the tau four-momentum in the event, while the neutrino from the W boson decay is reconstructed in the method as it would be for the e or μ + jets channel [25] by assuming the $t\bar{t}$ system is produced with no p_T.

Each probability is calculated by integrating over the differential cross section for the appropriate process:

$$P = \frac{1}{\sigma} \int d\sigma(\vec{y}) f(\tilde{q}_1) f(\tilde{q}_2) W(\vec{x}, \vec{y}) d\tilde{q}_1 d\tilde{q}_2, \qquad (1)$$

where $d\sigma$ is the differential cross section, f is the parton distribution function (PDF) for a quark with momentum fraction of the incident proton $\tilde{q}$, $\vec{x}$ refers to observed quantities, $\vec{y}$ refers to parton level quantities, and $W(\vec{x}, \vec{y})$ is the transfer function used to map $\vec{x}$ to $\vec{y}$ based on simulation studies. The event probability is a sum of the signal and background probabilities weighted by the signal and background fractions, respectively. To improve the statistical uncertainty on the M_{top} measurement, the likelihood function includes a Gaussian constraint on the background fraction set to 0.5 ± 0.1 from Table I. We evaluate the likelihood function for each of the 31 input top-quark masses and fit the result with a second-order polynomial to derive M_{top} and its statistical uncertainty. We calibrate the measurement on 21 simulated $t\bar{t}$ samples covering a mass range of 155 to 195 GeV/c^2. The likelihood function and fit for the data before applying the calibration functions can be seen in Fig. 2. We measure M_{top} to be 172.7 ± 9.3 (stat) GeV/c^2.

The largest systematic uncertainty comes from the JES and is calculated to be 3.4 GeV/c^2. We also consider systematic uncertainties from the differences in parton showering models (0.5 GeV/c^2), color reconnection (0.5 GeV/c^2), ISR and FSR (0.3 GeV/c^2), PDF's (0.1 GeV/c^2), and the uncertainty on the fraction of $t\bar{t}$ pairs produced from gg fusion (0.2 GeV/c^2). The background
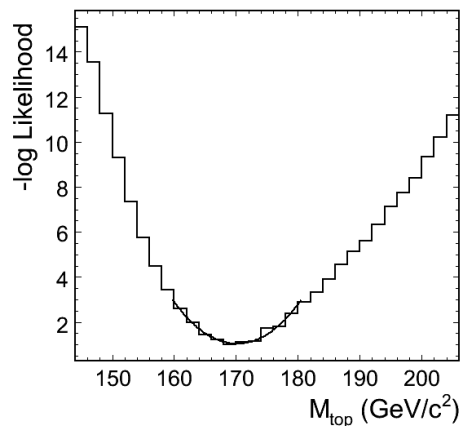

FIG. 2. Negative log of the top-quark mass likelihood as a function of M_{top} for all data events. The calibration functions have not yet been applied.

fraction uncertainty is measured by shifting each background source within its uncertainty from Table I (0.5 GeV/c^2). We consider uncertainties from different b-jet fragmentation models and semileptonic branching ratios for jets from b quarks as well as shifts in the energy scale of these jets (0.4 GeV/c^2). We also account for shifts from the tau energy scale (0.2 GeV/c^2). The pileup systematic uncertainty (1.0 GeV/c^2) accounts for a known mismodeling in the luminosity profile of the simulation. Uncertainty due to local non-linearity of the method and any assumptions used is estimated by shifting the calibration function within its uncertainty (0.2 GeV/c^2). We take the remaining 0.14 GeV/c^2 uncertainty on the fit of the mass residual (defined as the true mass subtracted from the measured mass) across all 21 mass points as an uncertainty on the limited size of the simulation sample. We find M_{top} to be 172.7 ± 9.3 (stat) ± 3.7 (syst) GeV/c^2 in agreement with the most recent Tevatron combination of 173.18 ± 0.94 GeV/c^2 [3].

Using data corresponding to an integrated luminosity of 2.2 fb^{-1}, we have made the first direct measurement of the top-quark mass in $t\bar{t}$ events identified as decaying to a hadronic τ + jets topology. Assuming a top-quark mass of 172.5 GeV/c^2, we find the $t\bar{t}$ pair production cross section to be 8.8 ± 3.3 (stat) ± 2.2 (syst + lumi) pb. This value is consistent with the next-to-next-to-leading order SM prediction [22] and recent measurements [28], including the D0 measurement in the same decay channel [6]. We measure the top-quark mass to be 172.7 ± 9.3 (stat) ± 3.7 (syst) GeV/c^2 in agreement with the Summer 2011 Tevatron top-quark mass combination of 173.18 ± 0.94 GeV/c^2 [3]. The measurements made in the τ + jets channel agree with current measurements and predictions, thus confirming lepton universality. Additionally, these measurements demonstrate that we can do complex analyses with tau leptons even in a high jet

multiplicity environment at hadron colliders. This is particularly interesting at the LHC where new physics, e.g. SUSY, could preferentially lead to final states with tau leptons.

[1] G. Aad *et al.* (ATLAS Collaboration), Eur. Phys. J. C **71**, 1 (2011).
[2] S. Chatrchyan *et al.* (CMS Collaboration), J. High Energy Phys. 07 (2011) 049.
[3] T. Aaltonen *et al.* (CDF Collaboration, D0 Collaboration), (2012), arXiv:1207.1069 [hep-ex].
[4] D. Hare, Ph.D. thesis, Rutgers University, FERMILAB-THESIS-2011-30 (2011).
[5] A. Abulencia *et al.* (CDF Collaboration), J. Phys. G: Nucl. Part. Phys. **34**, 245 (2007).
[6] V.M. Abazov *et al.* (D0 Collaboration), Phys. Rev. D **82**, 071102 (2010).
[7] A. Elagin, P. Murat, A. Pranko, and A. Safonov, Nucl. Instrum. Methods A **654**, 481 (2011).
[8] CDF uses a (z, ϕ, θ) coordinate system with the z-axis in the direction of the proton beam; ϕ and θ are the azimuthal and polar angle, respectively. The pseudorapidity is defined as $\eta = -\ln(\tan\frac{\theta}{2})$, and the transverse momentum and energy as $p_{\mathrm{T}} = p\sin\theta$ and $E_{\mathrm{T}} = E\sin\theta$, respectively. Missing transverse energy ($\not{E}_{\mathrm{T}} = |\vec{\not{E}}_{\mathrm{T}}|$) is defined as $\vec{\not{E}}_{\mathrm{T}} = -\sum_i E_{\mathrm{T}}^i \hat{\mathbf{n}}_{\mathbf{i}}$ where $\hat{\mathbf{n}}_{\mathbf{i}}$ is a unit vector in the transverse plane that points from the beam-line to the ith calorimeter tower.
[9] T. Aaltonen *et al.* (CDF Collaboration), Phys. Rev. Lett. **103**, 221801 (2009).
[10] F. Abe *et al.* (CDF Collaboration), Phys. Rev. D **45**, 1448 (1992).
[11] A. Bhatti *et al.*, Nucl. Instrum. Methods A **566**, 375 (2006).
[12] D. Acosta *et al.* (CDF collaboration), Phys. Rev. D **71**, 052003 (2005).
[13] A. Abulencia *et al.* (CDF Collaboration), Phys. Rev. Lett. **96**, 011802 (2006).
[14] T. Sjöstrand, P. Edén, C. Friberg, L. Lönnblad, G. Miu, S. Mrenna, and E. Norrbin, Comp. Phys. Commun. **135**, 238 (2001).
[15] R. Brun, R. Hagelberg, M. Hansroul, and J. Lassalle, CERN-DD-78-2-REV.
[16] E. Gerchtein and M. Paulini, (2003), arXiv:physics/0306031.
[17] Z. Was, Nucl. Phys. Proc. Suppl. **98**, 96 (2001).
[18] J. Alwall, P. Demin, S. de Visscher, R. Frederix, M. Herquet, F. Maltoni, T. Plehn, D. L. Rainwater, and T. Stelzer, J. High Energy Phys. 09 (2007) 028.
[19] M. L. Mangano, M. Moretti, F. Piccinini, R. Pittau, and A. D. Polosa, J. High Energy Phys. 07 (2003) 001.
[20] J. M. Campbell and R. Ellis, Phys. Rev. D **60**, 113006 (1999).
[21] B. Harris, E. Laenen, L. Phaf, Z. Sullivan, and S. Weinzierl, Phys. Rev. D **66**, 054024 (2002).
[22] S. Moch and P. Uwer, Nucl. Phys. Proc. Suppl. **183**, 75 (2008).
[23] P.Z. Skands and D. Wicke, Eur. Phys. J. C **52**, 133 (2007).
[24] S. Klimenko, J. Konigsberg, and T. Liss, FERMILAB-FN-0741 (2003).
[25] T. Aaltonen *et al.* (CDF Collaboration), Phys. Rev. D **84**, 071105 (2011).
[26] G. Mahlon and S. Parke, Phys. Rev. D **53**, 4886 (1996).
[27] F. Berends, H. Kuijf, B. Tausk, and W. Giele, Nucl. Phys. B **357**, 32 (1991).
[28] T. Aaltonen *et al.* (CDF Collaboration), Phys. Rev. Lett. **105**, 012001 (2010).